

A novel Newmark-based method applied to an anisotropic damage phase field model

Marco Lúcio Bittencourt¹, Carlos Lamarca Carvalho Sousa Esteves¹, Ana Luísa Evaristo Rocha Petrini¹, Rodrigo Santos Nogueira Júnior¹, José Luiz Boldrini¹

¹*Dept. of Integrated Systems, School of Mechanical Engineering, State University of Campinas, Campinas-SP
Mendeleev St. 200, 13083-860, SP, Brazil
mlb@fem.unicamp.br, c212012@dac.unicamp.br, analuisa.petrini@gmail.com, r244027@dac.unicamp.br,
josephbold@gmail.com*

Abstract. We present an anisotropic phase field model for fracture that uses a fourth-order tensor field to describe the damage that degrades the material's elasticity. The governing equations were obtained based on the use of the principle of virtual power (PVP), the balance of energy and the Clausius-Duhem inequality for the entropy. Small deformation isothermal case was considered. A failure criteria is also presented to define fracture and to establish a numerical criterion for damage irreversibility. The model was implemented using the finite element method (FEM) for the case of plane stress. Results are presented using two time integration methods for the motion equation: the standard and a modified Newmark method. The backward Euler method was used for the damage equation. Time efficiency and accuracy of results were compared for both Newmark methods.

Keywords: Phase field, Anisotropic damage, Fracture

1 Introduction

The general concept of mechanical damage is the degradation of the material properties relative to its original values (Mozaffari and Voyiadjis [1]). Since materials are not perfect, some damage is developed when subjected to any type of loading. One of the challenges of engineering is to take into consideration the damaging process of materials and properly design around it Scherer et al. [2].

The inherent discontinuous aspect of fracture is another issue that has been tackled by many different approaches (Svolos et al. [3]). The continuum damage dynamics (CDD) has been developed based on continuum dynamics to model and predict damage in materials. Most notably, the use of phase field methods to convert a discontinuous phenomena into a continuous one and common models consider that the level of damage in the continuum can be represented by a scalar variable (Zhuang et al. [4]). In such models, the degradation is given by an evolution equation which takes into account the loading conditions and the initial material properties. To analyze different directions or different damage phenomena (like fatigue), multiple scalar fields have been used as in Nguyen et al. [5].

In the present work, we numerically implemented a thermodynamically consistent phase field model which considers that the material degradation due to the damaging process is given by a fourth-order tensor. The model is simplified for the situation of plane stress in brittle materials and implemented using the FEM with quadrilateral elements and full Gaussian integration. Specifically, two methods were considered when solving the motion equation: the standard and a modified Newmark methods. Their efficiency and results are presented and compared.

2 Damage phase field

Following Boldrini et al. [6] and considering \mathbb{G} to be the fourth-order damage tensor, the initial boundary value problem to be solved is given by the following equations

$$\begin{aligned}
 \rho \ddot{\mathbf{u}} &= \text{div}((\mathbb{G} : \mathbb{C}_0 : \mathbb{G}) : \mathbf{E}) - \text{div}(g_c \gamma \nabla \mathbb{G} :: \nabla \mathbb{G}) + \text{div}(\hat{\mathbf{b}}\mathbf{D}), \\
 \dot{\hat{\mathbb{G}}} &= -\hat{F}(\mathbf{E} \otimes (\mathbb{C}_0 : \mathbb{G} : \mathbf{E}))^s - \hat{F} \frac{g_c}{\gamma} (\mathbb{G} - \mathbb{I}_s) + \hat{F} g_c \gamma \text{div}(\nabla \mathbb{G}).
 \end{aligned} \tag{1}$$

where \mathbf{u} is the displacement vector field, \mathbb{C}_0 is the elasticity fourth-order tensor of the virgin material, \mathbf{E} is the second order strain tensor field for small deformations, g_c is the Griffith fracture energy, γ is a parameter related to the width of the crack path, \mathbf{D} is the symmetric part of the velocity gradient, \mathbb{I}_s is the fourth-order symmetric identity tensor, \hat{F} is a kinematic factor related to the rate of damage evolution, and \hat{b} is a dynamic parameter related to mechanical damping. Given that \mathbb{G} is a fourth-order tensor, its gradient, $\nabla\mathbb{G}$, is a fifth order tensor and the four dots operation is defined by

$$\nabla\mathbb{G} :: \nabla\mathbb{G} = G_{ijkl,m}G_{ijkl,n} = A_{mn}. \quad (2)$$

We now consider the hypothesis of plane stress state such that there are no components of stress, strain or damage in the out of plane direction except for ε_{33} , which is merely a consequence of the Poisson's effect rather than an independent variable (the dependence and consideration of ε_{33} is necessary to properly represent the plane stress condition as shown by Li et al. [7]). Due to the major and minor symmetries of \mathbb{G} and the plane stress hypothesis, we can reduce the number of unknown components to six, namely G_{1111} , G_{2222} , G_{1212} , G_{1122} , G_{1112} , and G_{1222} . This means that each mesh node has two degrees of freedom for the displacement and six for the damage.

2.1 Failure criterion

Usually, scalar-based phase field models use a variable with range from zero to one to describe the transition between the virgin and the fractured material. The question then becomes: at which value of damage can we consider that failure has occurred? One way is to assume a reference value for the phase field variable from which material loses enough elasticity and no longer offers significant resistance to deformation.

When using a fourth-order tensor variable, the same criterion can not be applied to each of the tensor components as the local damage is given by the combination of the components. Therefore, a new failure criterion is needed to describe when there is enough damage in such a way that the elasticity matrix offers little resistance to applied loads. Let $\mathbb{C}^* = \mathbb{G} : \mathbb{C}_0 : \mathbb{G}$ be the degraded elasticity tensor. We can obtain its eigenvalues and calculate their geometric mean, $\zeta^{(n)}$, as

$$\zeta^{(n)} = (\lambda_1^{(n)}\lambda_2^{(n)}\lambda_3^{(n)})^{1/3}, \quad n = 0, 1, \dots, N, \quad (3)$$

where n is the time-step and $\lambda_i^{(n)}$ the eigenvalues at time-step n . The failure criterion adopted in this work is the relative geometric mean of the degraded elasticity's eigenvalues, ζ_r^n , defined by

$$\zeta_r^{(n)} = \frac{\zeta^{(n)}}{\zeta^{(0)}}. \quad (4)$$

As $\zeta_r^{(n)}$ tends to zero in a specific node, it is considered to be reaching failure in some direction. This scalar field can be used analogously to the scalar phase field variable to indicate the local damage as $\zeta_r^{(n)}$ also ranges from 0 (fractured) to 1 (virgin). This means that we can also use $\zeta_r^{(n)}$ to impose an irreversibility criterion, that is, to guarantee that no damaged node can recuperate/heal any existing damage. In that case, we only have to guarantee that $\dot{\zeta}_r^{(n)} \leq 0$.

3 Numerical implementation

Before applying a time integration method, we need to obtain and approximate by the FEM the weak forms of both equations given in eq. (1) so that we can discretize in time. The fourth-order damage tensor was reduced to a vector form and we need only to multiply both equations with vector test functions, \mathbf{w}_u and \mathbf{w}_g , and then integrate by parts in the domain as

$$\begin{aligned} \rho \int_{\Omega} \ddot{\mathbf{u}} \cdot \mathbf{w}_u &= - \int_{\Omega} ((\mathbb{G} : \mathbb{C}_0 : \mathbb{G}) : \mathbf{E}) : \nabla \mathbf{w}_u + g_c \gamma \int_{\Omega} (\nabla\mathbb{G} :: \nabla\mathbb{G}) : \nabla \mathbf{w}_u - \hat{b} \int_{\Omega} \mathbf{D} : \nabla \mathbf{w}_u + \text{B.T.}_1, \\ \int_{\Omega} \dot{\mathbb{G}} \cdot \mathbf{w}_g &= -\hat{F} \int_{\Omega} (\mathbf{E} \otimes (\mathbb{C}_0 : \mathbb{G} : \mathbf{E}))^s \cdot \mathbf{w}_g - \hat{F} \frac{g_c}{\gamma} \int_{\Omega} (\mathbb{G} - \mathbb{I}_s) \cdot \mathbf{w}_g - \hat{F} g_c \gamma \int_{\Omega} \nabla\mathbb{G} : \nabla \mathbf{w}_g + \text{B.T.}_2, \end{aligned} \quad (5)$$

where B.T.₁ and B.T.₂ are the boundary terms resulting from the divergence theorem. For the solving scheme, we assume that damage is delayed in time compared to the motion equation and uses the current strain on the damage equation. This allows to solve the motion equation first and use its result to obtain the current damage. If we discretize eq. (5) at the current time and reorganize their terms, we obtain the following expressions in matrix form

$$\begin{aligned} \rho \int_{\Omega} \mathbf{N}_u \hat{\mathbf{w}}_u^e \cdot \mathbf{N}_u \hat{\mathbf{u}}^e &= - \int_{\Omega} \mathbf{B}_u \hat{\mathbf{w}}_u^e [\mathbb{G}^*] \mathbf{B}_u \hat{\mathbf{u}}^e + g_c \gamma \int_{\Omega} \mathbf{B}_u \hat{\mathbf{w}}_u^e \cdot \{ \nabla \mathbb{G} :: \nabla \mathbb{G} \} - \hat{b} \int_{\Omega} \mathbf{B}_u \hat{\mathbf{w}}_u^e \cdot \mathbf{B}_u \hat{\mathbf{u}}^e, \\ \int_{\Omega} \mathbf{N}_g \hat{\mathbf{w}}_g^e \cdot \mathbf{N}_g \hat{\mathbb{G}}^e &= - \hat{F} \int_{\Omega} \mathbf{N}_g \hat{\mathbf{w}}_g^e [\mathbf{M}] \mathbf{N}_g \hat{\mathbb{G}}^e - \hat{F} \frac{g_c}{\gamma} \int_{\Omega} \mathbf{N}_g \hat{\mathbf{w}}_g^e \cdot \mathbf{N}_g \hat{\mathbb{G}}^e + \hat{F} \frac{g_c}{\gamma} \int_{\Omega} \mathbf{N}_g \hat{\mathbf{w}}_g^e \cdot \{ \mathbf{d} \} - \\ &\quad \hat{F} g_c \gamma \int_{\Omega} \mathbf{B}_g \hat{\mathbf{w}}_g^e \cdot \mathbf{B}_g \hat{\mathbb{G}}^e, \end{aligned} \quad (6)$$

where B.T.₁ and B.T.₂ are assumed zero for simplicity, \mathbf{N}_u and \mathbf{N}_g are the matrices of shape functions, \mathbf{B}_u and \mathbf{B}_g are the matrices of global derivatives of shape functions, \mathbf{d} is the vector form for \mathbb{I}_s , and \mathbf{M} is the resulting matrix from the term $(\mathbf{E} \otimes (\mathbb{C}_0 : \mathbb{G} : \mathbf{E}))^s$ after factoring out the components of \mathbb{G} . The terms in brackets are obtained separately in the full tensor form and then reduced to the adequate equivalent matrix for the plane stress case.

Remembering that the nodal coefficients of the approximations of the functions and the displacement, velocity and acceleration of the motion equation and the damage variable, they can be factored out of the integral sign, and the following equations results for each element e

$$\begin{aligned} \mathbf{M}_u^{(e)} \hat{\mathbf{u}}^{(e)} + \mathbf{K}_v^{(e)} \hat{\mathbf{u}}^{(e)} + \mathbf{K}_u^{(e)} \hat{\mathbf{u}}^{(e)} &= \mathbf{w}_a^{(e)}, \\ \mathbf{M}_g^{(e)} \hat{\mathbb{G}}^{(e)} + (\mathbf{Q}_g^{(e)} + \hat{F} \frac{g_c}{\gamma} \mathbf{M}_g^{(e)} + \mathbf{K}_g^{(e)}) \hat{\mathbb{G}}^{(e)} &= \mathbf{w}_b^{(e)}, \end{aligned} \quad (7)$$

where the element matrices are given by

$$\begin{aligned} \mathbf{M}_u^{(e)} &= \rho \int_{\Omega} \mathbf{N}_u^T \mathbf{N}_u, \quad \mathbf{K}_v^{(e)} = \hat{b} \int_{\Omega} \mathbf{B}_u^T \mathbf{B}_u, \\ \mathbf{K}_u^{(e)} &= \int_{\Omega} \mathbf{B}_u^T [\mathbb{G}^*] \mathbf{B}_u, \quad \mathbf{w}_a^{(e)} = g_c \gamma \int_{\Omega} \mathbf{B}_u^T \{ \nabla \mathbb{G} :: \nabla \mathbb{G} \}, \\ \mathbf{M}_g^{(e)} &= \int_{\Omega} \mathbf{N}_g^T \mathbf{N}_g, \quad \mathbf{Q}_g^{(e)} = \hat{F} \int_{\Omega} \mathbf{N}_g^T [\mathbf{M}] \mathbf{N}_g, \\ \mathbf{K}_g^{(e)} &= \hat{F} g_c \gamma \int_{\Omega} \mathbf{B}_g^T \mathbf{B}_g, \quad \mathbf{w}_b^{(e)} = \hat{F} \frac{g_c}{\gamma} \int_{\Omega} \mathbf{N}_u^T \mathbf{d}. \end{aligned} \quad (8)$$

After computing the element matrices, a global system is obtained to solve for all the nodal displacements and the damage terms. For the time integration, the backward Euler scheme was adopted for the damage equation and two options of the Newmark methods were considered for the motion equation.

3.1 Backward Euler method for the damage equation

For the damage equation, at the current time $n + 1$, we can write the global system as

$$\mathbf{M}_g \dot{\mathbb{G}}^{(n+1)} + (\mathbf{Q}_g^{(n+1)} + \hat{F} \frac{g_c}{\gamma} \mathbf{M}_g + \mathbf{K}_g) \mathbb{G}^{(n+1)} = \mathbf{w}_b, \quad (9)$$

where $\mathbf{Q}_g^{(n+1)}$ depends on the current displacement obtained from the motion equation and acts as the coupling term between the two equations. We can rewrite the rate of damage as

$$\dot{\mathbb{G}}^{(n+1)} = \frac{\mathbb{G}^{(n+1)} - \mathbb{G}^{(n)}}{\Delta t}, \quad (10)$$

where Δt is the time-step size adopted. Therefore, eq. (9) becomes

$$\left[\Delta t \mathbf{Q}_g^{(n+1)} + \left(1 + \hat{F} \Delta t \frac{g_c}{\gamma} \right) \mathbf{M}_g + \Delta t \mathbf{K}_g \right] \mathbb{G}^{(n+1)} = \Delta t \mathbf{w}_b + \mathbf{M}_g \mathbb{G}^{(n)}. \quad (11)$$

3.2 Newmark method for the motion equation

For the motion equation at the current time $n + 1$, we can write the global system as

$$\mathbf{M}_u \ddot{\mathbf{u}}^{(n+1)} + \mathbf{K}_v \dot{\mathbf{u}}^{(n+1)} + \mathbf{K}_u \mathbf{u}^{(n+1)} = \mathbf{w}_a^{(n)}. \quad (12)$$

The displacement and velocity vectors are approximated using parameters α and β as

$$\begin{aligned} \dot{\mathbf{u}}^{(n+1)} &= \dot{\mathbf{u}}^{(n)} + [(1 - \alpha)\ddot{\mathbf{u}}^{(n)} + \alpha\ddot{\mathbf{u}}^{(n+1)}]\Delta t, \\ \mathbf{u}^{(n+1)} &= \mathbf{u}^{(n)} + \dot{\mathbf{u}}^{(n)}\Delta t + [(0.5 - \beta)\ddot{\mathbf{u}}^{(n)} + \beta\ddot{\mathbf{u}}^{(n+1)}]\Delta t^2. \end{aligned} \quad (13)$$

Since the damage is delayed, the terms \mathbf{K}_u and \mathbf{w}_a dependent on \mathbb{G} are computed using the damage $\mathbb{G}^{(n)}$ from the previous step. We can express the acceleration $\ddot{\mathbf{u}}^{(n+1)}$ in terms of the displacement $\mathbf{u}^{(n)}$ from eq. (13)(b). The resulting expression is replaced in eq. (13)(a) to write the velocity $\dot{\mathbf{u}}^{(n+1)}$ in terms of the displacement vector $\mathbf{u}^{(n+1)}$. Both expressions are replaced in eq. (12) and the following system of equations are obtained for $\mathbf{u}^{(n+1)}$:

$$\begin{aligned} \left(\frac{1}{\beta\Delta t^2} \mathbf{M}_u + \frac{\alpha}{\beta\Delta t} \mathbf{K}_v + \mathbf{K}_u^{(n)} \right) \mathbf{u}^{(n+1)} &= \mathbf{M}_u \left(\frac{1}{\beta\Delta t^2} \mathbf{u}^{(n)} + \frac{1}{\beta\Delta t} \dot{\mathbf{u}}^{(n)} + \left(\frac{1}{2\beta} - 1 \right) \ddot{\mathbf{u}}^{(n)} \right) + \\ &\mathbf{K}_v \left(\frac{\alpha}{\beta\Delta t} \mathbf{u}^{(n)} + \left(\frac{\alpha}{\beta} - 1 \right) \dot{\mathbf{u}} + \left(\frac{\alpha}{2\beta} - 1 \right) \Delta t \ddot{\mathbf{u}} \right) + \mathbf{w}_a^n. \end{aligned} \quad (14)$$

To achieve unconditional stability and second order accuracy, the standard Newmark method adopts $\beta = 0.5$ and $\alpha = 0.25$. The following coefficients are defined:

$$\begin{aligned} a_1 &= \frac{1}{\beta\Delta t^2}, & a_2 &= \frac{\alpha}{\beta\Delta t}, & a_3 &= \frac{1}{\beta\Delta t}, \\ a_4 &= \frac{1}{2\beta} - 1, & a_5 &= \frac{\alpha}{\beta} - 1, & a_6 &= \left(\frac{\alpha}{2\beta} - 1 \right) \Delta t. \end{aligned} \quad (15)$$

From them, eq. (14) is rewritten as

$$\left(a_1 \mathbf{M}_u + a_2 \mathbf{K}_v + \mathbf{K}_u^{(n)} \right) \mathbf{u}^{(n+1)} = \mathbf{M}_u \left(a_1 \mathbf{u}^{(n)} + a_3 \dot{\mathbf{u}}^{(n)} + a_4 \ddot{\mathbf{u}}^{(n)} \right) + \mathbf{K}_v \left(a_2 \mathbf{u}^{(n)} + a_5 \dot{\mathbf{u}}^{(n)} + a_6 \Delta t \ddot{\mathbf{u}}^{(n)} \right) + \mathbf{w}_a^n. \quad (16)$$

3.3 Modified Newmark method for the motion equation

The proposed method in this work is another way of solving eq. (12) based on a fixed point strategy. We can see from eq. (13) that both approximations are given in terms of the current acceleration $\ddot{\mathbf{u}}^{(n+1)}$ and we can define a predictor based only on the terms of the previous step, n , for the current sub-iteration k as

$$\begin{aligned} \tilde{\mathbf{u}}_k^{(n+1)} &= \dot{\mathbf{u}}^{(n)} + (1 - \alpha)\Delta t \ddot{\mathbf{u}}^{(n)}, \\ \tilde{\mathbf{u}}_k^{(n+1)} &= \mathbf{u}^{(n)} + \dot{\mathbf{u}}^{(n)}\Delta t + (0.5 - \beta)\Delta t^2 \ddot{\mathbf{u}}^{(n)}. \end{aligned} \quad (17)$$

To correct the velocity and displacement vectors for time-step $n + 1$, we can add the contribution of the updated acceleration as

$$\begin{aligned}\dot{\mathbf{u}}^{(n+1)} &= \tilde{\mathbf{u}}_k^{(n+1)} + \alpha \Delta t \ddot{\mathbf{u}}_k^{(n+1)}, \\ \mathbf{u}^{(n+1)} &= \tilde{\mathbf{u}}_k^{(n+1)} + \beta \Delta t^2 \ddot{\mathbf{u}}_k^{(n+1)}.\end{aligned}\quad (18)$$

If we consider the predictors of eq. (17), we can rewrite eq. (12) as

$$\mathbf{M}_u \ddot{\mathbf{u}}_k^{(n+1)} = \mathbf{w}_a^n - \mathbf{K}_v \tilde{\mathbf{u}}_k^{(n+1)} - \mathbf{K}_u^{(n)} \tilde{\mathbf{u}}_k^{(n+1)}.\quad (19)$$

Using a nodal basis and a lumped mass matrix, the solution of the previous system of equations is trivial.

After solving for the current acceleration, we can update the displacement and velocity using eq. (18). The convergence criterion used was the norm of the increment of the displacement, that is, if $\|\beta \Delta t^2 \ddot{\mathbf{u}}_k^{(n+1)}\| \leq \epsilon$ then convergence was achieved. We used $\epsilon = 10^{-8}$ and about 2 sub-iterations were needed for convergence.

This modified version of the Newmark method is conditionally stable. The values of $\beta = 0.516$ and $\alpha = 0.145$ were determined to obtain the stability region and at least second order accuracy. The maximum time-step size is obtained by

$$\Delta t_{\max} \leq \frac{1.96}{\Omega_{\text{neq}}},\quad (20)$$

where $\Omega_{\text{neq}} = \sqrt{\lambda_{\text{neq}}}$ and λ_{neq} is the maximum eigenvalue obtained from the generalized eigenvalue problem $\mathbf{K}^{(e)} - \lambda \mathbf{M}^{(e)} = 0$, where $\mathbf{K}^{(e)}$ and $\mathbf{M}^{(e)}$ are the stiffness and mass matrices of the smallest element.

Therefore, this modified version becomes more suitable when using high-order elements, since the increased degrees of freedom won't increase significantly the time necessary to solve the system of equations. Since a more refined mesh would lead to a smaller Δt_{\max} , one can use a coarser mesh with high-order elements to compensate in accuracy and give a result with better quality. For this initial study, however, only first order elements were used to show the validity of the proposed approach.

4 Results

For the results, the material used was cast iron with properties $\rho = 7300 \text{ kg/m}^3$, $\gamma = 0.00025 \text{ m}^2$, $g_c = 2700 \text{ N/m}$, Young's modulus $E = 200 \text{ GPa}$, and Poisson's coefficient $\nu = 0.24$. Additionally, $\hat{F} = 1 \text{ m}^2\text{s/kg}$ and $\hat{b} = 0 \text{ kg/(m s)}$. The considered case was a square plate clamped at the bottom edge and subjected to a nodal positive constant velocity, $v_0 = 0.005 \text{ m/s}$, at the upper edge as shown in Figure 1. Since this analysis is mostly qualitative, a coarse mesh with 100 elements is used.

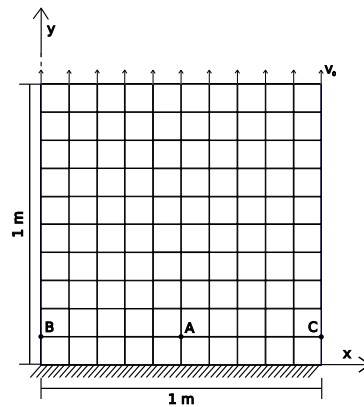


Figure 1. Mesh, boundary and loading conditions for the considered example.

Following the restrictions of stability on eq. (20), a time-step of 9×10^{-6} s was used for the modified Newmark. For the sake of comparison, the same time-step was adopted for the standard Newmark. The final time of analysis was 1 s. In this particular example, despite not having any notches, failure is expected to start from either nodes B or C. This is because the Poisson effect creates an elastic “necking” on the first row of elements which acts as a stress concentration factor leading to failure. The smaller the elements in the first row are, the closer to the clamped edge the failure starts.

Figure 2 shows the values of ζ_r for both methods over time at point A. Both methods have nearly identical behavior up until the moment of failure which happens at slightly different times.

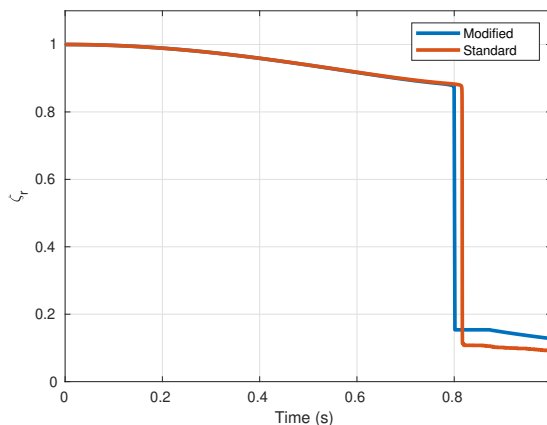


Figure 2. Evolution of ζ_r for the standard and modified Newmark method.

First, it can be seen that ζ_r only decreases over time as expected from the irreversibility criterion. The sudden drop observed in both results is the graphical representation of when the failure happened. At this point, the degradation provided by \mathbb{G} is enough for the material to lose most of its elasticity. In both scenarios, after the damage reached a certain level, it quickly decreased to a minimum value in very few time-steps, as expected for brittle failure.

Note that ζ_r never actually reaches zero even after failure. Since in this model there’s no re-meshing to visually show the separation of the elements where failure occurs, this great loss of elasticity is the equivalent of depicting the separation. Interestingly, having a node with zero elasticity leads to numerical errors and many authors choose to add a small increment to the damage variable to prevent that from happening. In this model, there’s no need for this correction since the other directions prevent the damage tensor from reaching $\zeta_r = 0$.

Figure 3 shows the distribution of ζ_r before, during and after the failure for the standard and modified Newmark methods. It can be seen that ζ_r properly indicates the progression of the crack propagation and that the obtained results are consistent.

5 Conclusions

The proposed modified Newmark method using a predictor-corrector scheme provided consistent results when compared to the standard version of the Newmark method. Despite requiring a smaller time-step size to achieve stability, it allowed transforming the left-hand side matrix into a diagonal matrix which greatly accelerated processing time.

Since solving a diagonal linear system is trivial, this allows the possibility to use high-order elements. Even with the increased number of degrees of freedom from using higher-order elements, there will not be significant increase when solving the system making it more efficient and giving higher quality results than the standard Newmark.

This version has good convergence properties just as the standard Newmark method. Since the damage equation depends on the current displacement, solving the motion equation with accuracy allows for a better description of the damage in the analysis.

Acknowledgements. The authors would like to thank the National Council for Scientific and Technological De-

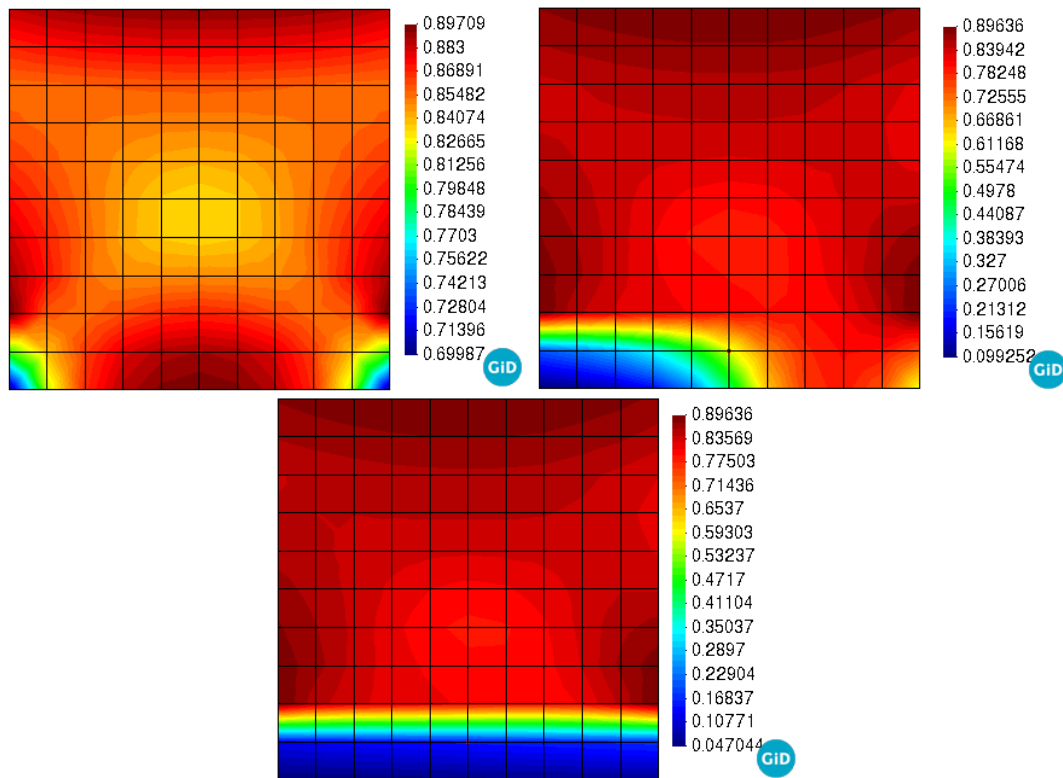


Figure 3. Evolution of ζ_r .

velopment (CNPq), Brazil under grant 140214/2022-4 for their support and the Coordenação de Aperfeiçoamento de Pessoal Superior - Brazil (CAPES) - Finance Code 001 for their support. The author Rodrigo S. N. Júnior was supported by grant #2021/11577-3, São Paulo Research Foundation (FAPESP).

Authorship statement. The authors hereby confirm that they are the sole liable persons responsible for the authorship of this work, and that all material that has been herein included as part of the present paper is either the property (and authorship) of the authors, or has the permission of the owners to be included here.

References

- [1] N. Mozaffari and G. Z. Voyiadjis. Phase field based nonlocal anisotropic damage mechanics model. *Physica D: Nonlinear Phenomena*, vol. 308, pp. 11–25, 2015.
- [2] J.-M. Scherer, S. Brach, and J. Bleyer. An assessment of anisotropic phase-field models of brittle fracture. *Computer Methods in Applied Mechanics and Engineering*, vol. 395, 2022.
- [3] L. Svolos, H. M. Mourad, G. Manzini, and K. Garikipati. A fourth-order phase-field fracture model: Formulation and numerical solution using a continuous/discontinuous galerkin method. *Journal of the Mechanics and Physics of Solids*, vol. 165, 2022.
- [4] X. Zhuang, S. Zhou, G. Huynh, P. Areias, and T. Rabczuk. Phase field modeling and computer implementation: A review. *Engineering Fracture Mechanics*, vol. 262, 2022.
- [5] T.-T. Nguyen, J. Réthoré, J. Yvonnet, and M.-C. Baietto. Multi-phase-field modeling of anisotropic crack propagation for polycrystalline materials. *Computational Mechanics*, vol. 60, pp. 289–314, 2017.
- [6] J. Boldrini, E. Barros de Moraes, L. Chiarelli, F. Fumes, and M. Bittencourt. A non-isothermal thermodynamically consistent phase field framework for structural damage and fatigue. *Computer Methods in Applied Mechanics and Engineering*, vol. 312, pp. 395–427. Phase Field Approaches to Fracture, 2016.
- [7] Z. Li, Y. Shen, F. Han, and Z. Yang. A phase field method for plane-stress fracture problems with tension-compression asymmetry. *Engineering Fracture Mechanics*, vol. 257, 2021.